

Takuro Hirai · Kayoko Namura · Takeo Kimura
Tetsuji Tsujino · Akio Koizumi

Lateral resistance of anchor-bolt joints between timber sills and foundations III: numerical simulations of the effect of sill thickness on the effective lateral resistance of multiple anchor-bolt joints

Received: July 6, 2005 / Accepted: October 5, 2005 / Published online: February 24, 2006

Abstract Effective lateral resistance of multiple anchor-bolt joints was estimated by considering sill thickness or length/diameter ratios of anchor bolts. Load–slip relationships of single anchor bolt joints were analyzed by the stepwise linear approximation based on the generalized theory of a beam on an elastic foundation and the criterion of “fracture bearing displacement” for several sill thicknesses or length/diameter ratios of anchor bolts. Monte Carlo simulations of the effective lateral resistance of multiple anchor-bolt joints were conducted using the analyzed load–slip curves of single anchor-bolt joints. Effective resistance ratios of multiple anchor-bolt joints were simulated for some combinations of length/diameter ratios of anchor bolts, lead-hole clearances, and number of anchor bolts. The simulated results are: (1) the influence of lead-hole clearance becomes more apparent as length/diameter ratios of single anchor-bolt joints decrease; (2) there is no obvious effect of number of anchor-bolts over the range of 5 to 15; (3) average effective resistance ratios can be adopted for allowable stress design; and (4) reduction of effective resistance ratios should be considered particularly for small length/diameter ratios of anchor-bolt joints.

Key words Multiple anchor-bolt joints · Effective lateral resistance · Stepwise linear analysis · Beam on foundation · Monte Carlo simulation

T. Hirai (✉) · A. Koizumi
Graduate School of Agriculture, Hokkaido University, Kita 9 Nishi
9, Kitaku, Sapporo 060-8589, Japan
Tel. +81-11-706-2591; Fax +81-11-706-3636
e-mail: hirai@for.agr.hokudai.ac.jp

K. Namura
Tostem Co. Ltd., Nagareyama 270-0163, Japan

T. Kimura
Minamifuji Sangyo Co. Ltd., Yokohama 224-0057, Japan

T. Tsujino
Faculty of Education, Iwate University, Morioka 020-0066, Japan

Introduction

In the second report of this study series,¹ we made some Monte Carlo simulations on the effective lateral resistance of multiple anchor-bolt joints loaded parallel and/or perpendicular to the grain of timber sills using experimental load–slip curves of single anchor-bolt joints that were obtained in Part I of the study.² The experimental examinations in Part I and numerical simulations in Part II, however, covered only limited combinations of sill thickness of 95 mm and anchor bolts of 12 or 16 mm in diameter. Load–slip characteristics of bolted joints, particularly the ultimate slips of them, are known to vary in a wide range due to length/diameter ratios of bolts, which must affect the effective lateral resistance of multiple anchor-bolt joints as simulated in Part II. The conclusions of the second report, therefore, are only applicable to the above combinations of sills and anchor bolts.

The experimental determination of load–slip curves of various combinations of sills and anchor bolts, however, needs much time, labor, and expense. Therefore, in this study, we conducted numerical analyses of the effect of length/diameter ratios of single anchor-bolt joints on the effective resistance of multiple anchor-bolt joints.

Numerical analyses

Load–slip relationships of single anchor-bolt joints

Load–slip relationships of single anchor-bolt joints between timber sills and foundations were estimated by the stepwise linear analyses based on the generalized theory of a beam on an elastic foundation.^{3–5} A single anchor-bolt joint was divided into several thin layers as shown in Fig.1 and the following basic differential equation was applied to each layer.

$$\frac{d^4 y_i}{dx_i^4} - \frac{N_i}{E_s L_{si}} \cdot \frac{d^2 y_i}{dx_i^2} + 4\mu_i^4 y_i = 0 \quad (1)$$

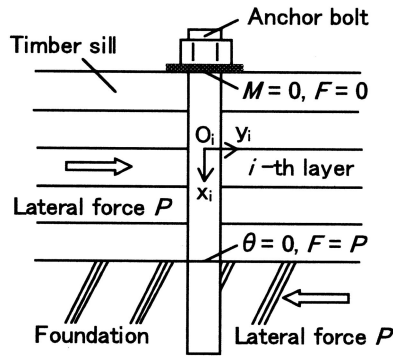


Fig. 1. Boundary conditions

where N_i = secondary axial force equilibrated with bearing force required to penetrate the washer into timber,

$E_s I_{si}$ = bending stiffness of the bolt in the i -th layer,

$$\mu_i = \sqrt[4]{\frac{k_{oi} d_i}{4E_s I_{si}}},$$

k_{oi} = bearing constant of timber in the i -th layer, and d_i = bolt diameter.

Boundary conditions were determined as shown in Fig. 1. That is, the anchor bolt was assumed to be fixed ($\theta = 0$) at the bottom surface of the sill. At the top surface of the sill, on the other hand, the bolt was assumed to be rotation free ($M = 0$). Semirigid behavior of the bolt head at the top surface of the sill^{6,7} was neglected to simplify the analyses. The anchor bolt considered in this study corresponded to one side of a symmetrical bolted joint with a steel center web plate.³⁻⁵

Bearing constants k_{oi} in Eq. 1 were determined in the following two ways. First, bearing stress–embedment curves from the origins to the maximum bearing stresses were calculated by the following empirical equation with two indexes: air-dry specific gravity r_u of timber and bolt diameter d , proposed for commercial softwood timber loaded parallel to the grain in a previous report.⁸

$$e = \frac{\sigma_b}{k_{oe}} - \frac{\gamma \sigma_{bm}}{k_{oni} \left[1 - \left(\frac{\sigma_b}{\gamma \sigma_{bm}} \right)^a \right]} \ln \left(1 - \frac{\sigma_b}{\gamma \sigma_{bm}} \right) + e_i \quad (2)$$

where σ_b = bearing stress (MPa), e = embedment (mm),
 $\sigma_{bm} = 91.35r_u - 11.15$ (MPa),

$$k_{oe} = \frac{1.647r_u + 0.372}{0.150d + 0.850} \times 10^2 \text{ (MPa/mm)}$$

$$k_{oni} = 4.119 \times 10^2 \text{ (MPa/mm)}, \gamma = 1.05, a = 4.4,$$

$$e_i = \frac{1}{2} \left(-c - 0.7604d + \sqrt{0.5782d^2 + 2dc + c^2} \right) \times 10^{-2}$$

(mm),

r_u = air-dry specific gravity of timber, d = bolt diameter

c = lead-hole clearance (mm).

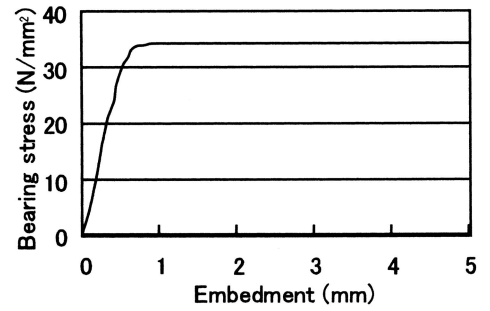


Fig. 2. Bearing stress–embedment curve for 12-mm bolts determined by bolt–wood bearing test

Second, the bearing stress–embedment curve shown in Fig. 2 for bolts of 12mm in diameter was directly determined by tension type bolt–wood bearing tests⁹ using timber specimens cut from undamaged parts of the sill specimens tested in Part I² to confirm the validity of the numerical analyses. Each bearing stress–embedment curve was replaced with seven successive segments of lines for stepwise linear analyses. Although the latter bearing constants determined by the bearing test gave better estimation of load–slip curves of single anchor-bolt joints as discussed later, the former bearing constants were adopted for calculating general or conservative load–slip relationships of single anchor-bolt joints.

Elastoplastic bending properties of anchor bolts were calculated by the following equation.^{3-5,10,11}

$$M = \frac{E_s r^4}{6\rho} \left[\frac{3}{2} k\pi + 3(1-k)\xi + (1-k)\phi(5-2)\phi^2 \sqrt{1-\phi^2} \right] \quad (3)$$

where M = bending moment, E_s = Young's modulus = 205 (GPa), $r = d/2$ = radius of bolt, ρ = radius of curvature, k = apparent ratio of strain hardening rate to the Young's modulus = 0.105, $\xi = \sin^{-1} \phi$, $\phi = \lambda/r$, λ = distance between the yield plane and the neutral plane, which is calculated from an apparent yield stress of 316 (MPa).

The apparent yield stress and the ratio of strain hardening rate to the Young's modulus were determined for approximating the bending moment–curvature curves of round bars of SS400 steel in the previous study,¹⁰ which did not show exact characteristics of the normal stress–strain relationship of SS400 steel.

The secondary axial force N_i was determined for each step of the calculation to be equilibrated with the bearing force required to penetrate the washer into timber. Embedment of the washer into timber was calculated from reduction of the projected length of the bent bolt. Bearing load–embedment curves between washers and sills were determined experimentally using commercial washers for bolts of 12mm in nominal or actual diameter. In preliminary tests, eccentric loads were applied as shown in Fig. 3 considering that washers were actually embedded with some inclination due to the slopes of bolt heads.^{3,6,7} The eccentricity e was roughly assumed to be 2.5mm by considering the rotational moment that gave trapezoidal

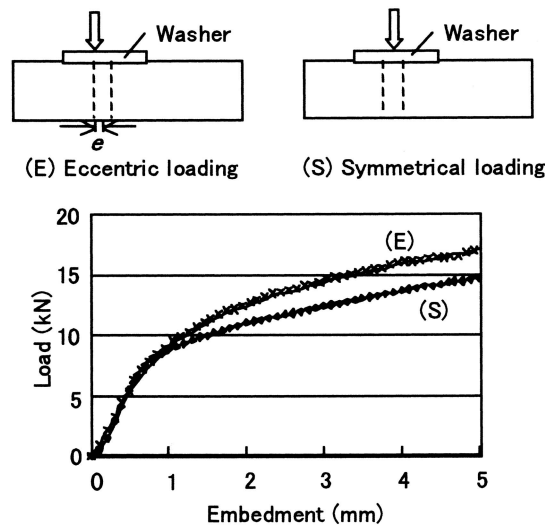


Fig. 3. Load-embedment curves between washers and sills

distributions of bearing displacements equivalent to the inclined depressions of tested timber under washers. The embedding resistance for eccentric loading was close to or greater than the resistance given by symmetrical loading as shown in Fig. 3. The effect of eccentric loading was also analyzed roughly by assuming a washer as a beam on an elastic foundation neglecting three-dimensional plate-bending action. It also showed that the inclination of a washer did not have a negative effect on the embedding resistance except for the reduction of effective contacted area resulting from separation of one side of the washer from the timber, which could be counted by considering displacement and slope of the washer in numerical analyses. From these preliminary considerations, the load-embedment curve (S) in Fig. 3 determined by symmetrical loading was used in the numerical analyses.

Anchor-bolt joints loaded parallel to the grain of sills were only taken into consideration because Part II¹ of our study showed that supplementary shares of anchor-bolt joints loaded perpendicular to the grain of sills were far less than those expected from the allowable lateral resistance of them.

Sill depths were assumed to be 38, 89, 105, and 120 mm, which were popular in Japanese light timber frame constructions and Japanese post and beam constructions. Bolt diameter and lead-hole clearance were assumed to be 12 mm and 0, 3, or 6 mm, respectively. The bearing load-embedment curves were calculated by substituting the bolt diameter and lead-hole clearance above and air-dry specific gravity $r_u = 0.45$ into Eq. 2.

In the stepwise linear analyses, an anchor-bolt joint was divided into 5 to 15 thin layers according to sill depth. These numbers of layers were determined from the examinations in the previous studies.^{3-5,10,11} Elastoplastic bending stiffness of the bolt and bearing constant of the sill were assumed to be constant in each layer on each step of the analyses.^{3-5,10,11} Frictional resistance between sills and foundations was first neglected to compare the calculated curves with the

experimental curves obtained in Part I² because the friction between timber and the steel support was lessened with oil in the tests. On the other hand, the frictional coefficient was provisionally assumed to be 0.3 for the calculation of load-slip curves used in the Monte Carlo simulations described later. The coefficient 0.3 was the static frictional coefficient between planed timber and steel,¹² which was a conservative estimation of the unknown frictional coefficient between timber and concrete surfaces.

Load-slip curves of single anchor-bolt joints were calculated stepwise up to the maximum lateral loads determined by the criterion, “fracture bearing displacement (FBD)”, proposed in the previous study.^{4,5,13-16} This criterion could indicate the maximum loads linked to critical splitting failures of timber members, but could not trace the load-slip behavior succeeding the maximum loads. Then, the load-slip relationships of single anchor-bolt joints after reaching maximum loads were approximated in the following two ways. First, single anchor-bolt joints were assumed to hold no lateral load after reaching maximum load (assumption 1). Second, load-slip relationships after reaching maximum load were approximated by declined linear segments with the slopes of one thirds the maximum loads from the test results of Part I² (assumption 2).

Monte Carlo simulation of effective lateral resistance of multiple anchor-bolt joints

Monte Carlo simulations were conducted on the effective lateral resistance of multiple anchor-bolt joints using the analyzed load-slip curves of single anchor-bolt joints. Statistical variance of load-slip curves of single anchor-bolts considered in Part II¹ was neglected in this study because the load-slip curves were calculated with no consideration for their variance. This assumption gives the ideal effective resistance ratio of 1.0 to any multiple anchor-bolt joint with no lead-hole clearance.

Sill thickness and lead-hole clearance was assumed to be 38, 89, 105, or 120 mm and 3 or 6 mm, respectively. A file of anchor-bolt joints loaded parallel to the sill grain was assumed to consist of 5, 10, or 15 anchor bolts. Load-slip curves of files of anchor-bolt joints were calculated 100 times per combination of sill thickness, lead-hole clearance, and number of anchor bolts. The effective resistance ratios of multiple anchor-bolt joints were determined from the simulated load-slip curves of files of anchor-bolt joints in the same way as presented in Part II.¹

Results and discussion

Analyzed load-slip curves of single anchor-bolt joints

The load-slip curves of single anchor-bolt joints analyzed neglecting the load-slip behavior after reaching maximum loads (assumption 1) are shown in Fig. 4 and those with

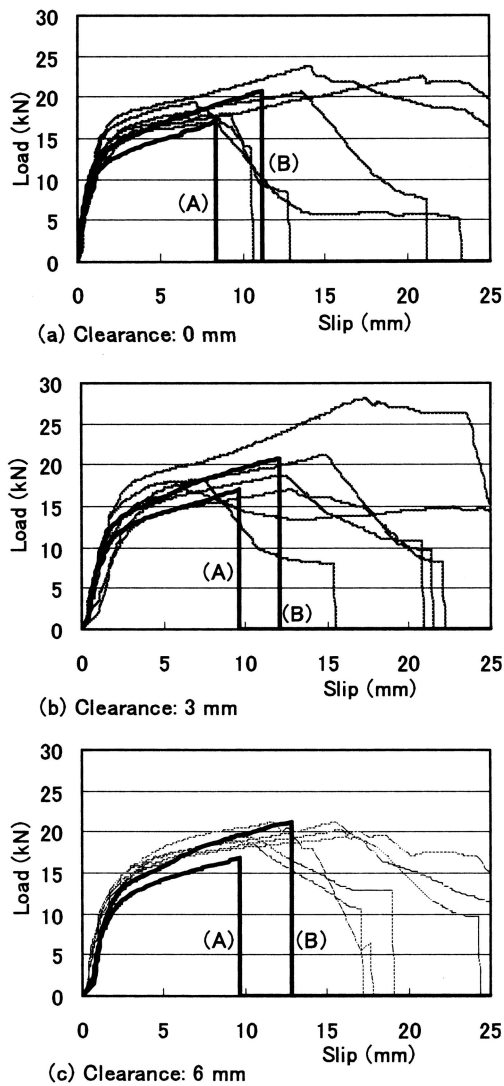


Fig. 4. Comparison of load-slip curves calculated by neglecting residual resistance after maximum loads with experimental curves for lead-hole clearances of **a** 0 mm, **b** 3 mm, and **c** 6 mm. *A*, Calculated from the bearing stress-embedment curve given by Eq. 2; *B*, calculated from the bearing stress-embedment curve shown in Fig. 2. *Thin lines* show experimental load-slip curves

approximated declined linear segments after maximum load (assumption 2) are shown in Fig. 5 with the experimental load-slip curves obtained in Part I.² The load-slip curves (*B*) in Figs. 4 and 5, which were analyzed based on the bearing stress-embedment curves directly determined by the bolt-wood bearing tests using matched specimens, gave better agreements with the experimental curves as a reasonable result. Less agreement between the experimental curves and the load-slip curves (*A*), which were analyzed based on the bearing stress-embedment curves given by empirical Eq. 2, might partially come from difference in moisture contents of timber specimens. That is, the average moisture content of timber specimens in Part I of the study and that of timber specimens used to determine Eq. 2 were

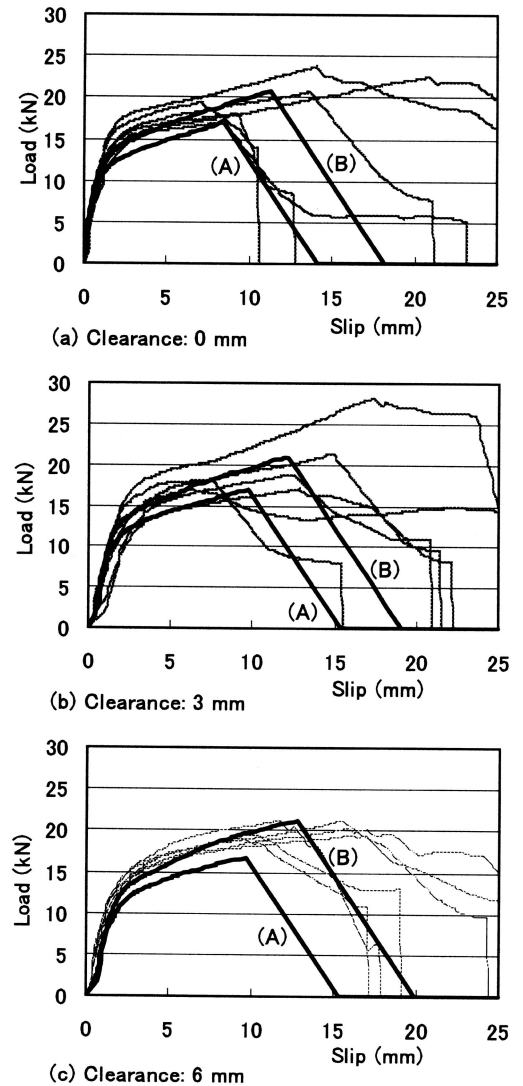


Fig. 5. Comparison of load-slip curves calculated by approximating residual resistance after maximum loads with experimental curves for lead-hole clearances of **a** 0 mm, **b** 3 mm, and **c** 6 mm. *A*, Calculated from the bearing stress-embedment curve given by Eq. 2; *B*, calculated from the bearing stress-embedment curve shown in Fig. 2. *Thin lines* show experimental load-slip curves

about 11% and 15%, respectively, and neither of the test results was standardized because of a lack of quantitative information about the effect of moisture content on bearing stress-embedment relationships.

The analyses based on the bearing stress-embedment curves determined with the matched specimens, however, do not give general estimations, but are only valid for particular specimen conditions. The bearing stress-embedment curves given with Eq. 2, therefore, were adopted for the Monte Carlo simulations as common or conservative estimations. Examples of load-slip curves of single anchor-bolt joints, which were calculated for a lead-hole clearance of 6 mm based on assumption 2, are shown in Fig. 6.

Simulated effective lateral resistance of multiple anchor-bolt joints

Figure 7 shows examples of the simulated load–slip curves of the files of anchor-bolt joints based on assumption 1 or 2, where each figure part a, b, c, or d, consists of ten curves randomly extracted from 100 simulated curves. Table 1

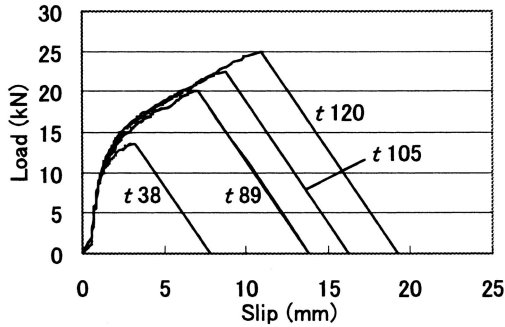
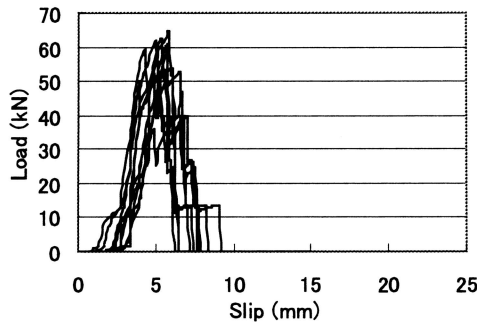


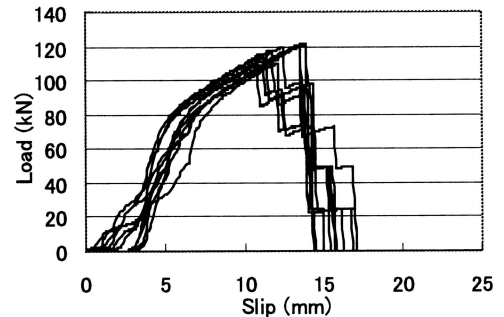
Fig. 6. Calculated load–slip curves for lead-hole clearance of 6 mm and sill thickness of 38, 89, 105, and 120 mm

shows the effective resistance ratios of average and fifth percentile lower limit lateral resistance of the files of five anchor-bolt joints to the ideal resistance simulated with assumption 1 and Table 2 shows those of the same files of anchor-bolt joints simulated with assumption 2. For sills that were 89, 105, or 120 mm thick, which corresponded to length/diameter ratios of 7.42, 8.75, or 10.0, respectively, there was little difference in the simulated effective resistance ratios between assumptions 1 and 2. These length/diameter ratios were equivalent to 14.84, 17.5, or 20.0 for bolted joints with single insert plates arranged symmetrically. For sills that were 38 mm thick with a length/diameter ratio of 3.17, which was equivalent to 6.34 for bolted joints with single insert plates arranged symmetrically, however, assumption 1 gave lower effective resistance ratios than assumption 2. This result means that the assumption of load–slip behavior or residual resistance after maximum load more clearly affects the effective lateral resistance of multiple anchor-bolt joints as the slips at maximum loads of single anchor-bolt joints become smaller. If the slips at maximum loads of single anchor-bolt joints are large enough to cover the variance of initial locations of

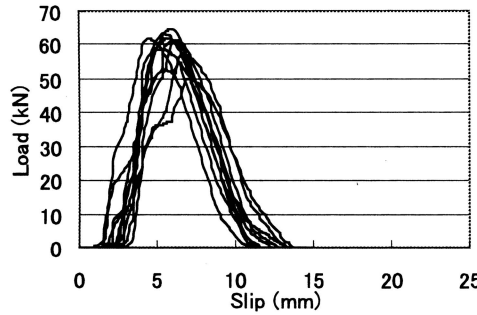
Fig. 7a–d. Examples of the simulated load–slip curves of files of five anchor-bolt joints of 12 mm in diameter and 6 mm in lead-hole clearance. **a** sill thickness 38 mm, assumption 1; **b** sill thickness 120 mm, assumption 1; **c** sill thickness 38 mm, assumption 2; **d** sill thickness 120 mm, assumption 2



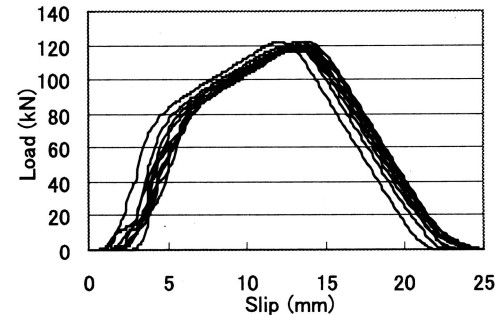
(a) Sill thickness = 38 mm, Assumption (1)



(b) Sill thickness = 120 mm, Assumption (1)



(c) Sill thickness = 38 mm, Assumption (2)



(d) Sill thickness = 120 mm, Assumption (2)

Table 1. Effective resistance ratios of average or fifth percentile lower limit resistance of the files of five anchor-bolt joints to the ideal resistance simulated by neglecting load–slip behavior after reaching maximum loads (assumption 1)

Sill thickness (mm)	38		89		105		120		
Lead-hole clearance (mm)	3	6	3	6	3	6	3	6	
Effective resistance ratio	Ave	0.94	0.77	0.96	0.94	0.98	0.94	0.98	0.96
	LL5	0.80	0.55	0.91	0.86	0.95	0.89	0.95	0.89

Diameter 12 mm; $n = 5$

Ave, average effective resistance ratio; LL5, fifth percentile lower limit effective resistance ratio

Table 2. Effective resistance ratios of average or fifth percentile lower limit resistance of the files of five anchor-bolt joints to the ideal resistance simulated by assuming declined linear segments of load–slip relationships (assumption 2)

Sill thickness (mm)	38		89		105		120		
Lead-hole clearance (mm)	3	6	3	6	3	6	3	6	
Effective resistance ratio	Ave	0.96	0.87	0.97	0.93	0.98	0.95	0.98	0.97
	LL5	0.91	0.73	0.95	0.88	0.96	0.89	0.96	0.91

Diameter 12 mm; $n = 5$

Table 3. Effective resistance ratios of average or fifth percentile lower limit resistance of the files of ten anchor-bolt joints to the ideal resistance simulated by assuming declined linear segments of load–slip relationships (assumption 2)

Sill thickness (mm)	38		89		105		120		
Lead-hole clearance (mm)	3	6	3	6	3	6	3	6	
Effective resistance ratio	Ave	0.95	0.85	0.97	0.93	0.98	0.94	0.98	0.96
	LL5	0.92	0.75	0.94	0.89	0.96	0.90	0.96	0.93

Diameter 12 mm; $n = 10$

Table 4. Effective resistance ratios of average or fifth percentile lower limit resistance of the files of 15 anchor-bolt joints to the ideal resistance simulated by assuming declined linear segments of load–slip relationships (assumption 2)

Sill thickness (mm)	38		89		105		120		
Lead-hole clearance (mm)	3	6	3	6	3	6	3	6	
Effective resistance ratio	Ave	0.95	0.86	0.97	0.92	0.98	0.93	0.97	0.96
	LL5	0.92	0.75	0.95	0.90	0.96	0.90	0.96	0.93

Diameter 12 mm, $n = 15$

multiple anchor-bolts, the load share of each anchor bolt at the maximum resistance of multiple anchor-bolt joints is distributed over a narrow range. In this case, there is no great difference in effective resistance ratio between the two assumptions because the residual resistance of each anchor bolt after reaching maximum load contributes little to the total resistance. If the slips at maximum loads of single anchor-bolt joints are small, on the other hand, load share of each anchor bolt at the maximum resistance is distributed over a wider range. In this case, the residual resistance of each anchor-bolt contributes greater. Of course the simulated energy capacities depend on the assumption of load–slip behavior, even for the anchor-bolt joints with large length/diameter ratios as shown in Fig. 7b, d.

For most anchor-bolt joints, reduction of initial stiffness within their allowable lateral resistance does not seem important because the frictional resistance due to vertical loads can prevent the slips due to horizontal forces even if the vertical components of earthquake forces decrease it to some extent. When we discuss the practical performance of other multiple connector joints, reduction of initial stiffness should be considered carefully. One of the rough estimations of initial stiffness may be given by assuming initial or offset slips to be halves of the lead-hole clearances and shifting the ideal load–slip curves counting them.

The declined linear segments of assumption 2 were determined only from the test results of single anchor-bolt joints with a sill thickness of 95 mm. Actual single anchor-bolt joints with thinner sills may lose lateral resistance immediately after splitting failures, which may result in some intermediate effective resistance ratios between the estimations shown in Tables 1 and 2. In Part II of this study series,¹ on the other hand, stricter simulations considering variation of load–slip curves gave comparatively higher effective resistance ratios than the simulations with definite load–slip curves. If we consider these factors overall, the effective resistance ratios of multiple anchor-bolt joints may be able to be roughly estimated with assumption 2. For more conservative or safe estimation, assumption 1 or average values of the resistance ratios simulated with assumptions 1 and 2 should be applied.

The effective resistance ratios of the files of 10 or 15 anchor-bolt joints simulated with assumption 2 are shown in Tables 3 or 4. Overview of Tables 2, 3, and 4 indicated that the lead-hole clearance exerted more influence as the length/diameter ratios of single anchor-bolt joints decreased. We found no obvious effect of the number of anchor bolts among the range of 5 to 15. From the tables, we can see that reduction of effective resistance ratios should

be considered particularly for small length/diameter ratios of anchor-bolt joints.

In this study, both average and fifth percentile lower limit effective resistance ratios were estimated. In ordinary allowable stress design, the allowable lateral resistance of single anchor-bolt joints is determined as the fifth percentile lower limit resistance of them. Then, the structural designers usually need the effective resistance ratio to the control resistance, which is calculated as the product of the allowable resistance and the number of anchor bolts. From this standpoint, we may reasonably be able to adopt the average effective resistance ratios shown in Tables 1–4 for allowable stress design, although it is not satisfactory if probability of failure is counted in structural design both directly and indirectly.

Conclusions

We numerically analyzed the load–slip relationships of single anchor-bolt joints based on the theory of a beam on an elastic foundation and FBD criterion. Using the analyzed load–slip curves, Monte Carlo simulations were conducted for timber sills that were 38, 89, 105 and 120 mm thick. The simulations gave the following conclusions:

1. Estimation of load–slip behavior of single anchor-bolt joints after reaching maximum load hardly affects the effective resistance of multiple anchor-bolt joints of large length/diameter ratios, but clearly affects if the slips at maximum loads of single anchor-bolt joints become smaller as the length/diameter ratios decrease.
2. The effect of lead-hole clearance becomes more apparent as the length/diameter ratios of single anchor-bolt joints decrease.
3. There is no obvious effect of the number of anchor bolts in the range of 5 to 15.
4. Average effective resistance ratios can be adopted for allowable stress design.
5. Reduction of effective resistance ratios should be considered particularly for small length/diameter ratios of anchor-bolt joints.

From conclusions 2 and 5, we propose:

1. Sill thickness/bolt diameter ratios should be designed to be as large as possible. We recommend them to be at least 7 or 8.
2. Lead holes should be bored as tight as construction work allows when thinner sills and/or thicker bolts are used.
3. The effective lateral resistance should be estimated conservatively counting the reduction up to 20%.

References

1. Hirai T, Namura K, Yanaga K, Koizumi A, Tsujino T (2006) Lateral resistance of anchor-bolt joints between timber sills and foundations II. Effective lateral resistance of multiple anchor-bolt joints. *J Wood Sci* DOI 10.1007/s10086-005-0739-2
2. Namura K, Yanaga K, Sasaki Y, Koizumi A, Hirai T (2005) Lateral resistance of anchor-bolt joints between timber-sills and foundations I. Single-shear tests of anchor-bolt joints of Japanese post and beam constructions (in Japanese). *Mokuzai Gakkaishi* 51:110–117
3. Hirai T (1990) Load–slip relationships of mechanical wood-joints with steel webs (in Japanese). *Res Bull Coll Exp For Hokkaido Univ* 47:215–248
4. Hirai T (1990) Some considerations on lateral resistance of mechanical wood-joints. *Proceedings of the 1990 International Timber Engineering Conference*, Tokyo pp 241–247
5. Hirai T (1991) Analyses of the lateral resistance of bolt joints and drift-pin joints in timber II. Numerical analyses applying the theory of a beam on an elastic foundation (in Japanese). *Mokuzai Gakkaishi* 37:1017–1025
6. Hunt R (1987) Mechanics of laterally loaded nail joints in timber. Report No. 393, Department of Civil Engineering, University of Auckland
7. Nishiyama N, Ando N (2003) Analysis of load–slip characteristics of nailed wood joints: application of a two-dimensional geometric nonlinear analysis. *J Wood Sci* 49:505–512
8. Hirai T (1989) Basic properties of mechanical wood-joints 2. Bearing properties of wood under a bolt (in Japanese). *Res Bull Coll Exp For Hokkaido Univ* 46:967–988
9. Hirai T (1989) Rational testing methods for determination of basic lateral resistance of bolted wood-joints (in Japanese). *Res Bull Coll Exp For Hokkaido Univ* 46:959–966
10. Hirai T (1983) Nonlinear load–slip relationship of bolted wood-joints with steel side-members II. Application of the generalized theory of a beam on an elastic foundation. *Mokuzai Gakkaishi* 29:839–844
11. Hirai T (1985) Nonlinear load–slip relationship of bolted wood-joints with steel side-members III. Advanced numerical analysis based on the generalized theory of a beam on an elastic foundation. *Mokuzai Gakkaishi* 31:165–170
12. Hirai T (1991) Effect of frictional resistance on lateral resistance of bolted timber-joints with steel side-webs (in Japanese). *Mokuzai Gakkaishi* 37:517–522
13. Hirai T (1991) Analyses of the lateral resistance of bolt joints and drift-pin joints in timber I. An assumption of cracking fracture criterion for mechanical timber-joints loaded parallel to the grain (in Japanese). *Mokuzai Gakkaishi* 37:1011–1016
14. Hirai T (1993) A Monte Carlo simulation of the effective lateral resistance of multiple bolted timber joints with lead hole clearances subjected to axial forces. *Mokuzai Gakkaishi* 39:1027–1035
15. Hirai T, Wakashima Y (1996) Lateral resistance and fracture modes of nailed timber joints III. Numerical analyses of maximum lateral resistance of nailed timber-plywood joints. *Mokuzai Gakkaishi* 42:1195–1201
16. Hirai T, Wakashima Y (1998) Lateral resistance of mechanical timber joints. *Proceedings of the 5th World Conference on Timber Engineering*, vol. 1, Montreux, pp 842–843